Int. J. Heat Mass Transfer. Vol. 34, No. 7, pp. 1773–1781, 1991
Printed in Great Britain

0017–9310/91 $3.00 + 0.00

Spectral dynamics of computer-simulated, two-dimensional, few-tube fluidized-bed combustors

S. L. CHANG, R. W. LYCZKOWSKI and G. F. BERRY
Argonne National Laboratory, Energy Systems Division, 9700 South Cass Avenue, Argonne, IL 60439, U.S.A.

(*Received* 6 *November* 1989 *and in final form* 30 *August* 1990)

Abstract—Argonne National Laboratory has developed methods for investigating erosion phenomena in fluid/solids systems by integrating a state-of-the-art, two-phase, two-dimensional, hydrodynamic computer model (FLUFIX, which computes temporal and spatial distributions) with erosion models that correlate the computed hydrodynamic properties with erosion patterns and rates. In this paper, a spectral analysis correlating the porosity, pressure, and velocity of a generic, few-tube, fluidized-bed combustor in time and space is reported. The major frequencies of porosity, pressure, and velocity oscillations are 0.7–4 Hz. Porosity and pressure oscillations traveled in the combustor at speeds of 0.4–1 m s^{-1}. Pressure oscillations are well correlated with the lagging porosity oscillations.

INTRODUCTION

FLUIDIZED-BED combustion (FBC) technology attracts intense commercial interest because of its ability to burn high-sulfur coal in an economical and environmentally acceptable manner, despite unsolved erosion problems [1]. Detailed knowledge of the complex phenomena of solids circulation and bubble motion in the bed through either experimental measurement or computer simulation is considered essential to understanding the erosion problems. Over the past few years, Argonne National Laboratory (ANL) has been developing methods to investigate local erosion in bubbling FBC systems [2], using a state-of-the-art, two-phase, two-dimensional, hydrodynamic computer model, FLUFIX, to compute temporal and spatial distributions of the flow properties [3] and using spectral analysis and erosion models to evaluate flow dynamics and local erosion patterns and rates [4].

Using these methods, ANL has conducted an erosion study on a generic two-dimensional, few-tube, fluidized-bed combustor [5–7]. The spectral analysis reported in this paper is part of the study. Spectral analysis for FBC applications [5, 8] examines how fluctuations of hydrodynamic properties are distributed around their average values and how adjacent fluctuations (adjacent in time or space) are related. The autocorrelation and its Fourier transform, the energy spectrum, show the relationship between adjacent property fluctuations, from which the major oscillation modes of the two-phase flow in the bed were determined. Because of the good cross-correlations between adjacent property fluctuations in space, the fluctuation propagation speeds were also determined. In addition, the phase diagrams of property fluctuations and their rates of change were used to demonstrate the periodicity of randomness of the fluctuations.

FORMULATION

The FLUFIX code computes temporal and spatial distributions of flow properties in an FBC, yielding the hydrodynamic properties of a two-phase flow based on the basis of the principles of conservation of mass and momentum [3]. The general mass conservation equations and the separated phase momentum equations for transient and isothermal gas/solids non-reactive multiphase flow (in vector notation and conservation law form) for the hydrodynamic model are:

continuity

$$\frac{\partial}{\partial t}(\varepsilon_k \rho_k) + \nabla \cdot (\varepsilon_k \rho_k \mathbf{v}_k) = 0; \tag{1}$$

momentum

$$\underbrace{\frac{\partial}{\partial t}(\varepsilon_k \rho_k \mathbf{v}_k) + \nabla \cdot (\varepsilon_k \rho_k \mathbf{v}_k \mathbf{v}_k)}_{\text{Acceleration}} = \underbrace{\nabla \cdot \bar{\bar{\sigma}}_{ke}}_{\text{Stress}} + \underbrace{\varepsilon_k \rho_k \mathbf{g}}_{\text{Gravity}} + \underbrace{\sum_{i=1}^{n} \bar{\beta}_{ik}(\mathbf{v}_i - \mathbf{v}_k)}_{\text{Interphase drag}}. \tag{2}$$

The effective stress tensor, $\bar{\bar{\sigma}}_{ke}$, contains pressure, viscous, and Coulombic components according to the convention

$$\nabla \cdot \bar{\bar{\sigma}}_{ke} = -(1-\delta_{ks_i})\nabla \cdot (P\bar{\bar{I}}) + \nabla \cdot (\varepsilon_k \bar{\bar{\tau}}_{kv}) - \delta_{ks_i} \nabla \cdot \bar{\bar{\tau}}_{kc}. \tag{3}$$

NOMENCLATURE

A	power spectral density	δ	Kronecker delta function
c	constant	ε	gas volume fraction or porosity
f	fluctuations	ε_k	volume fraction of phase k
G	solids elastic modulus [Pa]	ε_s	solids volume fraction, $1-\varepsilon$
G_0	constant	ε^*	compaction gas volume fraction
g	fluctuation	λ	time lag [s]
$\mathbf{g}$	acceleration due to gravity [m s^{-2}]	μ_k	microscopic viscosity [Pa·s × 10 = poise]
$\bar{\bar{I}}$	unit tensor	ρ_k	density of phase k [kg m^{-3}]
P	pressure [Pa]	$\bar{\bar{\sigma}}_{kc}$	effective stress [Pa]
t	time [s]	$\bar{\bar{\tau}}_{kc}$	Coulombic stress for solids [Pa]
U_{mf}	minimum fluidizing velocity [m s^{-1}]	$\bar{\bar{\tau}}_{kv}$	microscopic viscous phase stress tensor [Pa]
V	velocity [m s^{-1}]	ω	angular frequency [rad s^{-1}].
$\mathbf{v}$	velocity [m s^{-1}].		

Greek symbols

		Subscripts	
α_f	standard deviation	i	phase
β_f	autocorrelation	k	phase
β_{fg}	cross-correlation	n	total number of phases
$\bar{\bar{\beta}}_{ik}$	fluid–particle friction coefficient tensor [kg m^{-3} s^{-1}]	s	phase.

The Kronecker delta function is given by

$$\delta_{ks_i} = 1 \quad \text{if} \quad k = s_i$$
$$\delta_{ks_i} = 0 \quad \text{if} \quad k \neq s_i \tag{4}$$

where $k = s_i$ indicates a solids phase. The momentum equations (equations (2) and (3)) were first given in ref. [9] and extended in ref. [10].

The solids elastic modulus, $G(\varepsilon_k)$, is defined as the normal component of the solids Coulombic stress through the following relationship:

$$\nabla \cdot \bar{\bar{\tau}}_{kc} = G(\varepsilon_k)\bar{\bar{I}} \cdot \nabla \varepsilon_k. \tag{5}$$

For convenience, $G(\varepsilon_k)$ is the only component of the solids Coulombic stress used. A simple semi-empirical formula of the solids elastic modulus may be written for a two-phase fluid/solids mixture ($s_i = s$) as

$$G(\varepsilon_s)/G_0 = \exp\left[c(\varepsilon_s - \varepsilon_s^*)\right] = \exp\left[-c(\varepsilon - \varepsilon^*)\right]. \tag{6}$$

In this study, the constants c and G_0 were taken to be 600 and 1 Pa, respectively; the value of ε^* was 0.367.

The two-phase FLUFIX code computes temporal and spatial distributions of porosity, pressure, and velocity for numerous computational nodes in an FBC. A tremendous volume of data is generated. To efficiently and effectively compare and evaluate these results, statistical parameters such as mean, variance, autocorrelation, power spectral density, and cross-correlation were used. The mean value of a property distribution, $F(t)$, is defined as follows:

mean

$$\bar{F} = \frac{1}{T}\int_{t_0}^{t_0+T} F(t)\,\mathrm{d}t \tag{7}$$

where t_0 is an arbitrary initial time and T the time interval of computation. The interval T is arbitrary, but it must be long compared with the fluctuation period. The fluctuation of a property function, $f(t) = F(t) - \bar{F}$, represents the instantaneous deviation from the mean value. Standard deviation, autocorrelation, and power spectral density of a fluctuation are defined as follows [11]:

standard deviation

$$\alpha_f = [\overline{f(t)f(t)}]^{1/2}; \tag{8}$$

autocorrelation

$$\beta_f(\lambda) = \overline{f(t)f(t+\lambda)}/\alpha_f^2; \tag{9}$$

power spectral density

$$A(\omega) = \frac{2}{T}\int_0^T \beta_f(\lambda)\cos\omega\lambda\,\mathrm{d}\lambda. \tag{10}$$

The value of an autocorrelation coefficient, β_f, stands for the possibility of a periodic oscillation at a given location. If β_f is plotted against the time lag λ, a peak autocorrelation value at λ_0 often indicates an oscillation mode having a period equal to λ_0. The same oscillation mode is also identifiable in a plot of power spectral density vs frequency by the peak value at the corresponding frequency, $1/\lambda_0$. Most FBC property fluctuations have several oscillation modes. Note that turbulent fluctuations have no preferred

oscillation mode. Similar to an autocorrelation, the cross-correlation of two fluctuations f and g are defined as follows [11]:

cross-correlation

$$\beta_{f,g}(\lambda) = \overline{f(t)g(t+\lambda)}/(\alpha_f \alpha_g). \quad (11)$$

The cross-correlation represents the degree of similarity of two fluctuation patterns; the higher the cross-correlation value, the higher the degree of similarity. For two identical fluctuation patterns, the cross-correlation coefficient equals one. In general, if a high cross-correlation coefficient for two adjacent locations is found at a certain time lag, the fluctuations are regarded to propagate from one location to the other during a time period equal to the time lag. The propagation speed can be computed by dividing the spacing of the two locations by the time lag. In this paper, the propagation speeds were computed for cross-correlation peaks having values higher than 0.6. Because the fluctuations of pressure, porosity, and velocity are discrete data points computed from the FLUFIX code and stored (typically) every 50 time steps, statistical parameters (equations (7)–(11)) were integrated numerically using trapezoidal approximation.

FLUIDIZED-BED COMBUSTOR

The two-dimensional, few-tube FBC systems under investigation were 0.816 m high and 0.306 m wide and had an initial bed height of 0.442 m. The air was injected into the combustor through four inlets. Two different bed geometries were considered: five tubes in three rows (Fig. 1(a)) and three tubes in two rows. A computational grid of 48 by 18 nodes was defined for the FBC system. The locations of some typical nodes (e.g. nodes 2, 4, D–H, and d–h) are shown for one quarter of the three-node bed in Fig. 1(b). At each node, the FLUFIX code computed the temporal porosity, pressure, solids velocity, and gas velocity distributions. For the three-tube FBC, the total computational time included 1400 stored time steps (5 ms interval) for a total of 7 s: an initial 2 s period at a jet velocity of $1.12\times$ minimum fluidizing velocity ($U_{mf} = 20.9$ cm s^{-1}), a second 2.5 s period at $1.7U_{mf}$,

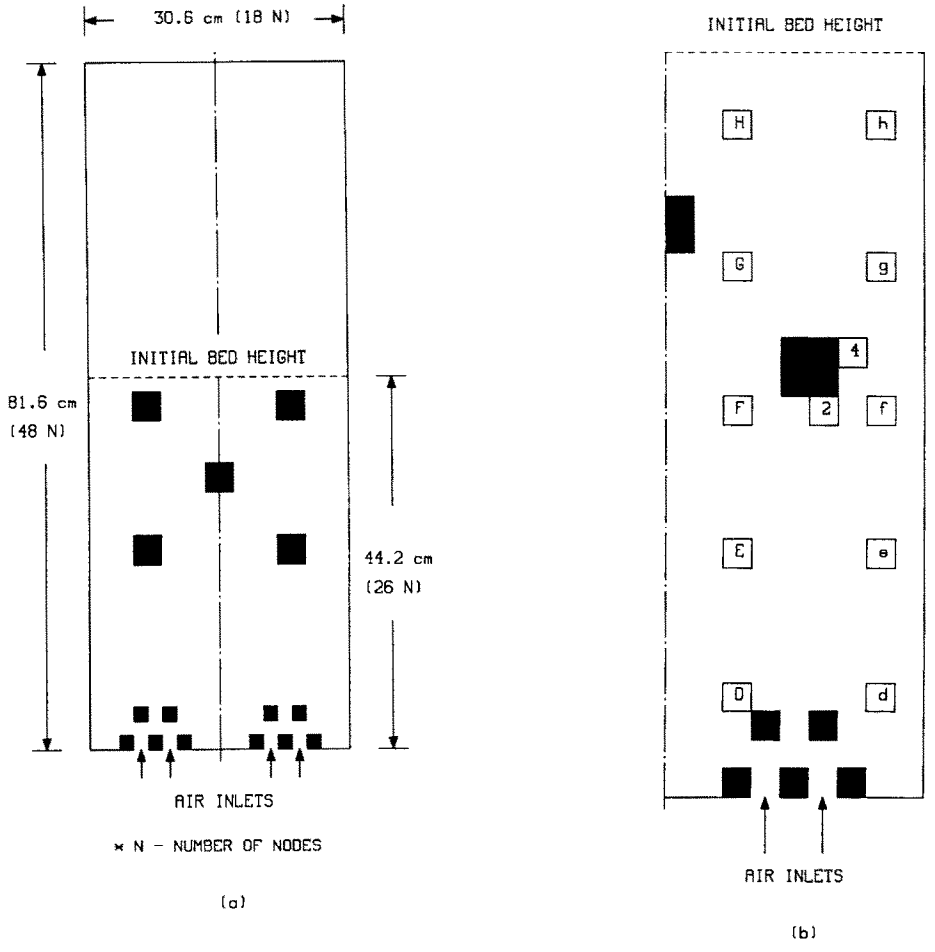

FIG. 1. (a) Generic five-tube FBC geometries. (b) Lower right quarter of a three-tube FBC showing some node locations.

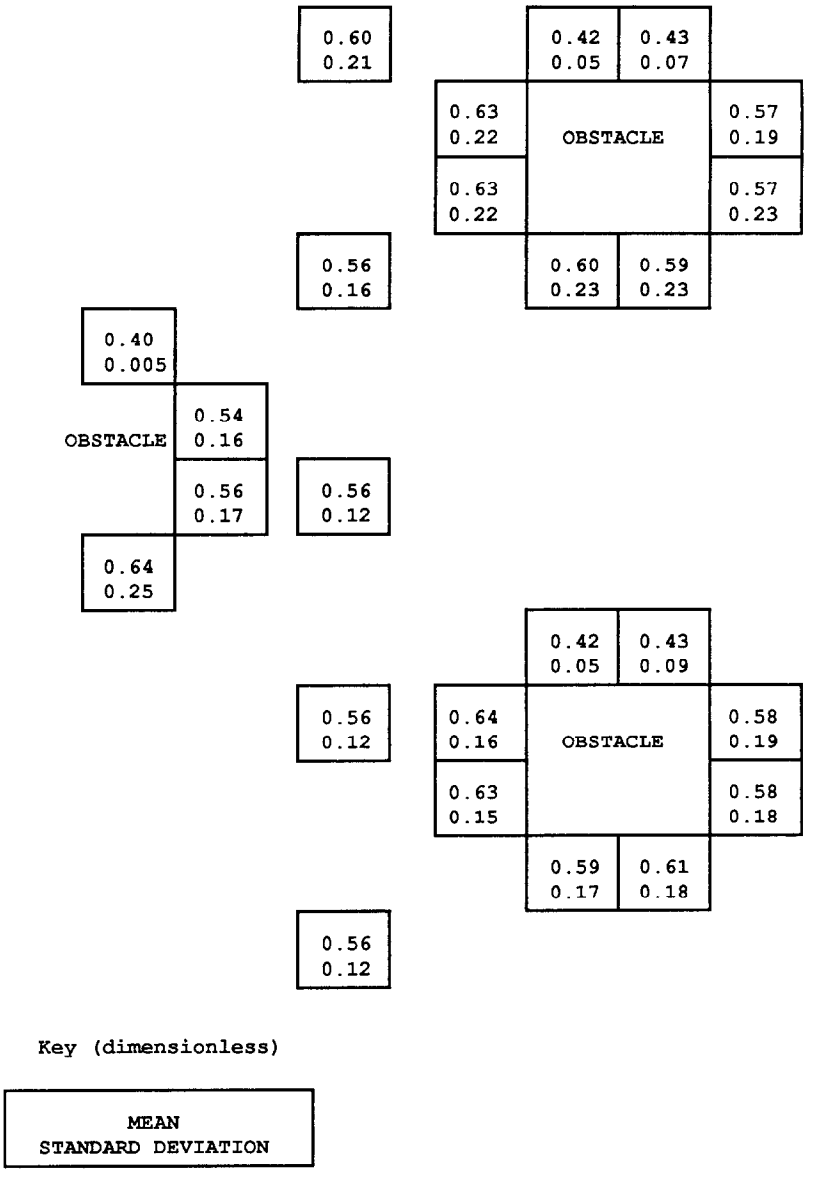

FIG. 2. Porosity means and standard deviations (five-tube; $2.3U_{mf}$).

and the last 2.5 s period at $2.3U_{mf}$. A similar time frame for the five-tube arrangement covered 2 s at $1.12U_{mf}$, 2.5 s at $1.7U_{mf}$, and 3 s at $2.3U_{mf}$.

RESULTS AND DISCUSSION

Two basic statistical parameters, the mean and standard deviation, were used to evaluate the bubble dynamics in the FBC. From a statistical point of view, a bubble (usually defined by an isoporosity value of 0.8) may have passed a location during a time interval if the sum of porosity mean and standard deviation at the location is larger than a specified value; the larger the sum, the larger the bubble. Some statistical means and standard deviations of porosity fluctuations from 4.5 to 7.5 s in a five-tube FBC are summarized in Fig. 2. These results were computed from 20 nodes around the tubes (called obstacles in Fig. 2) and five middle column nodes, D–H. The sum of porosity mean and standard deviation at many locations in the bed was higher than 0.8, indicating the active bubble motions. No bubble was found on top of the tubes, where the porosity mean was low (close to the packed bed porosity, $\varepsilon \sim 0.4$) and the standard deviation was near zero. The porosity mean and standard deviation around the tubes averaged about 0.55 and 0.16, respectively.

The means and standard deviations of porosity, pressure, and velocity were affected by the fluidizing velocity. The porosity means around the tubes gen-

crally increased with the jet velocity. For example, beneath the center tube of a three-tube FBC, the porosity mean increased from 0.55 to 0.66 as the jet velocity increased from $1.12U_{mf}$ to $2.3U_{mf}$. In other words, higher fluidizing velocities caused larger bubbles to form. The means and standard deviations of pressure fluctuations showed little sensitivity to the tube arrangement. For instance, the pressure means and standard deviations of the node beneath the center tube in a three-tube FBC were 3.60 and 0.49 kPa, respectively; their corresponding values in a five-tube FBC were 3.64 and 0.49 kPa.

Autocorrelations and power spectral densities of local porosity, pressure, velocity, and momentum flux fluctuations in an FBC were used to help determine major oscillation modes, if any. Major oscillation modes were determined by matching the autocorrelation peaks with the power spectral density peaks. Figure 3(a) shows a porosity fluctuation from 4.5 to 7 s at node 2 located beneath the side tube in the three-tube FBC (see Fig. 1(b)). Figure 3(b) is the autocorrelation vs time lag plot, and Fig. 3(c) the power spectral density vs frequency plot. The two autocorrelation peaks at time lags of 0.6 and 1.16 s matched the two power spectral density peaks at 1.7 and 0.9 Hz; thus, two major porosity oscillation modes at these frequencies were determined. In general: (1) the major oscillation modes for porosity, pressure, and velocity were 0.7–4 Hz; (2) a primary low frequency mode at about 1 Hz was found in most locations; and (3) the velocity fluctuations had higher frequency modes than porosity and pressure.

Figure 4 summarizes the major pressure oscillatory modes in a five-tube FBC at $2.3U_{mf}$. The primary oscillation mode was about 0.8 Hz and the secondary oscillation mode was 2.2 Hz. According to Broadhurst and Becker, the slugging frequency for this situation is about 1.4 Hz [12]; according to Verloop and Heertjes the major frequency is about 1.3 Hz [13]. The major frequencies estimated from these two theories are close to the primary oscillation mode we computed. Possible causes of these oscillations include bubble formation, breakup, and coalescence. The oscillation modes were insensitive to the fluidizing velocity and tube arrangement.

Fluctuations at different locations in space or different properties at the same location can sometimes be cross-correlated. The two porosity fluctuations in Fig. 5(a) at nodes D and E (locations are shown in Fig. 1(b)) were cross-correlated. Their cross-correlation and phase diagram are shown in Figs. 5(b) and (c). These two porosity fluctuations had a high cross-correlation coefficient, 0.8, at 0.105 s (Fig. 5(b)), and the phase diagram (Fig. 5(c)) shows the complexity of the correlation. Note that the phase diagram of two fluctuations is a straight line if the two fluctuations are identical and is a closed loop (ellipse) if two periodic functions have the same frequency. In general, porosity fluctuations at adjacent vertical locations had good similarity, and a propagation

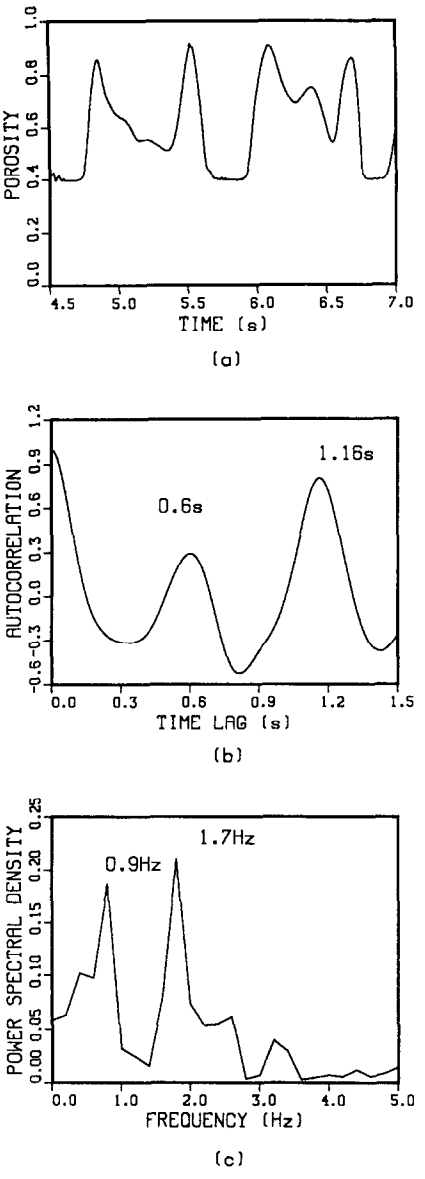

FIG. 3. Porosity fluctuations, autocorrelation, and power spectral density (node 2, three-tube, $2.3U_{mf}$): (a) fluctuations; (b) autocorrelation; (c) power spectral density.

speed could usually be determined from the cross-correlation plot. However, the porosity fluctuations at nodes d and e near the wall could not be correlated because the solids axial velocity at node d near the wall was nearly zero and could not be correlated with any other fluctuation. Table 1 summarizes porosity propagation velocities for three- and five-tube FBCs at $2.3U_{mf}$. Local propagation velocities (0.47–1.0 m s^{-1}) changed with location and with tube arrangement. The average propagation speed in a five-tube FBC was faster than a three-tube FBC. According to Grace's theory, the porosity propagation rate is about 1.16 m s^{-1} [14]; according to Needham and Merkin's

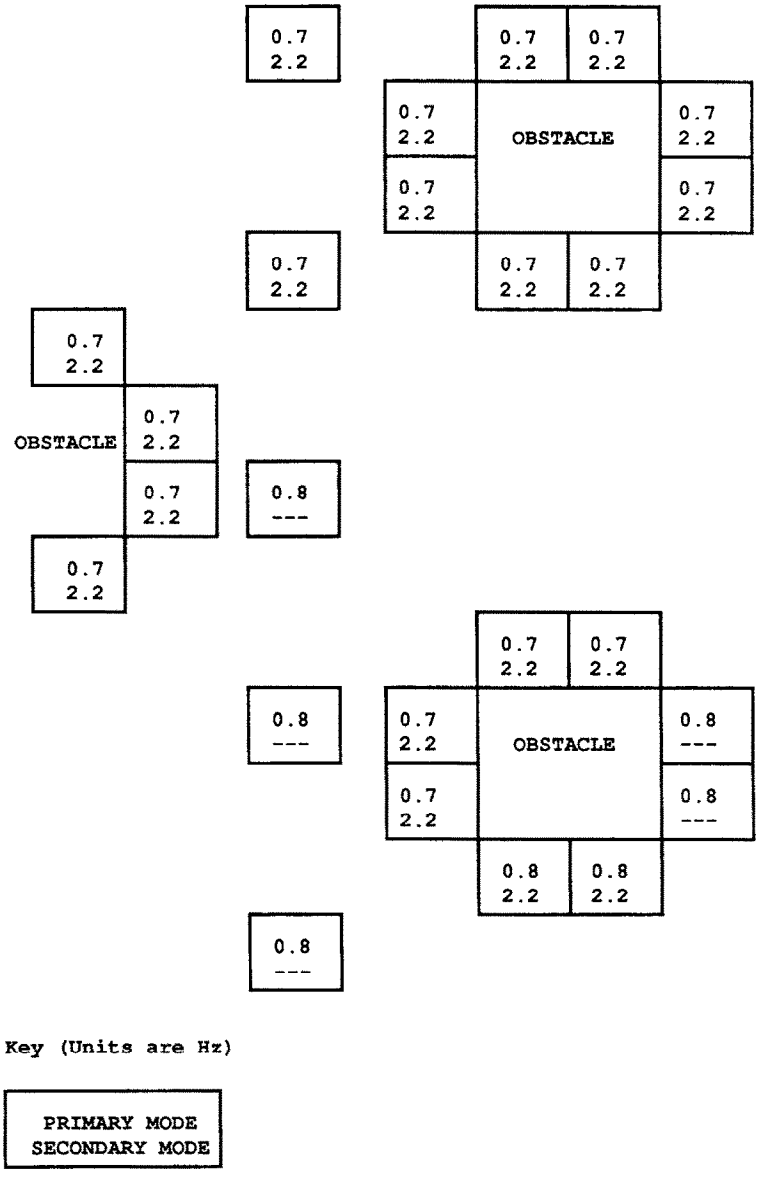

FIG. 4. Pressure oscillation modes (five-tube, $2.3U_{mf}$).

theory, the propagation speed is about 1.14 m s^{-1} [15]. These estimated propagation velocities agree closely with our results.

Besides the cross-correlations in space, cross-correlations between porosity and pressure, porosity and velocity, and pressure and velocity at the same location were performed. Only the pressure and the lagging porosity were well correlated. In the three-tube FBC, pressure and porosity fluctuations had about 64–84% similarity and the time lags were between 0.1 and 0.38 s. These important findings indicate that simple diagnostic measurements of pressure can be used to correlate erosion patterns.

Finally, phase diagrams were constructed in an attempt to evaluate the oscillatory behavior and possible fluctuation randomness. A porosity fluctuation at node 4 in the upper right-hand side of the side tube in the three-tube FBC, from 4.5 to 7 s and its phase diagram are shown in Fig. 6. The porosity varied from 0.38 to 0.9 and the rate of change ranged from -20 to 10 s^{-1}. The two large loops in Fig. 6(b) indicate that two large bubbles passed this location. Several smaller loops in the center region show the oscillations of the bubble itself. Fluctuations appear to have a certain degree of randomness. By accumulating a much longer computational time period, the present study may be extended to the chaotic analysis of the FBC.

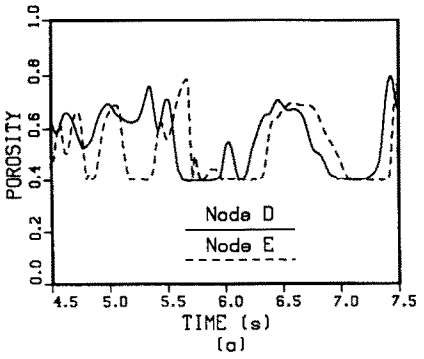

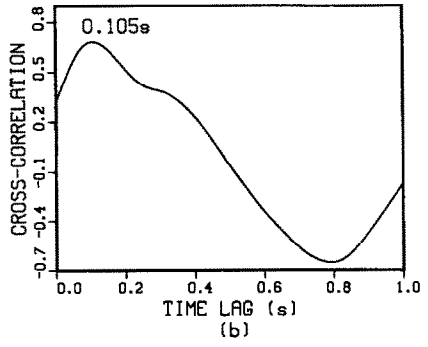

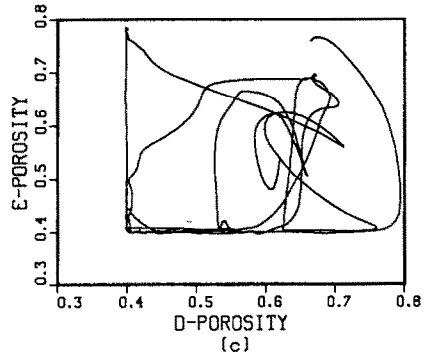

FIG. 5. Cross-correlation between two-porosity fluctuations and phase diagram (nodes d and 4, five-tube, $2.3U_{mf}$): (a) porosities; (b) cross-correlation; (c) phase diagram.

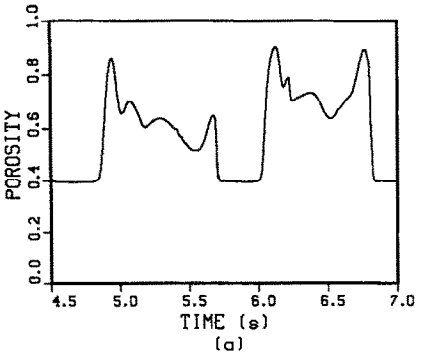

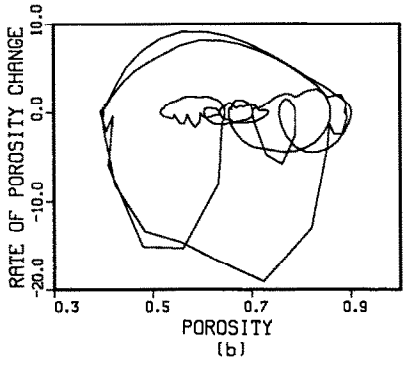

FIG. 6. Porosity fluctuation and its phase diagram at node 4: (a) porosity; (b) phase diagram.

CONCLUSIONS

Spectral analysis, including the calculation of statistical parameters (i.e. mean, standard deviation, autocorrelation, cross-correlation, and power spectral density) and the construction of phase diagrams, was conducted to study the flow dynamics of a few-tube FBC. The results provide much information toward developing correlations of the hydrodynamics and erosion in a few-tube FBC. Porosity means and standard deviations appear to be useful in describing bubble motions. Major oscillation modes (0.7–4 Hz) of porosity, pressure, and gas and solids velocities were found in most locations in the bed. Fluctuations of pressure, porosity, and velocity generally had good cross-correlation, and they propagated from the bottom of the bed with speeds of 0.4–1.0 m s^{-1}. As for the cross-correlation between the pressure and the lagging porosity fluctuations, the high cross-correlation values (over 0.6) supported the use of simple diagnostic measurements of pressure to correlate

Table 1. Propagation velocity of porosity fluctuations ($2.3U_{mf}$)

Porosity propagation velocity (m s^{-1})					
Middle column			Side column		
Nodes	Three-tube	Five-tube	Nodes	Three-tube	Five-tube
D–E	0.50	0.81	d–e	—	—
E–F	0.74	0.59	e–f	0.85	1.00
F–G	0.85	1.00	f–g	0.47	0.68
G–H	0.89	0.94	g–h	0.47	0.81
Average	0.75	0.84	Average	0.60	0.83

bubble dynamics and erosion patterns. However, the differences in the distribution of pressure and porosity means and standard deviation suggest careful interpretation of the pressure measurements is required. Despite the different instantaneous flow patterns in a three- and a five-tube FBC, the similar statistical results indicated that a three-tube FBC simulation may provide adequate information about the flow dynamics of a generic few-tube FBC.

Acknowledgements—This work was performed for U.S. Department of Energy, Morgantown Energy Technology Center, Contract W-31-109-Eng-38, and for the Electric Power Research Institute under the cooperative R&D venture 'Erosion of FBC Heat Transfer Tubes'.

REFERENCES

1. J. Stringer, Current information on metal wastage in fluidized-bed combustors. *Proc. Ninth Int. Conf. on Fluidized-bed Combustion* (Edited by J. P. Mustonen), Vol. 2, pp. 685–696. American Society of Mechanical Engineers, New York (1987).
2. R. W. Lyczkowski, J. X. Bouillard, G. F. Berry and D. Gidaspow, Erosion calculations in a two-dimensional fluidized bed, *Proc. Ninth Int. Conf. on Fluidized Bed Combustion* (Edited by J. P. Mustonen), Vol. 2, pp. 697–706. American Society of Mechanical Engineers, New York (1987).
3. R. W. Lyczkowski and J. X. Bouillard, Interim user's manual for FLUFIX/MOD1: a computer program for fluid solids hydrodynamics, Argonne National Laboratory Report ANL/EES-TM-361, Argonne, Illinois (October 1986).
4. R. W. Lyczkowski, S. Folga, S. L. Chang, J. X. Bouillard, C. S. Wang, G. F. Berry and D. Gidaspow, State-of-the-art computation of dynamics and erosion in fluidized bed tube banks, *Proc. Tenth Int. Conf. on Fluidized Bed Combustion*, Vol. 3, pp. 465–479. American Society of Mechanical Engineers, New York (1988).
5. S. L. Chang, R. W. Lyczkowski and G. F. Berry, Spectral analysis of dynamics in fluidized bed tube banks. In *Multiphase Transport and Particulate Phenomena* (Edited by T. Nejat Veziroglu), pp. 407–418. Hemisphere, New York (1989).
6. R. W. Lyczkowski, S. Folga, S. L. Chang and J. X. Bouillard, Computation of dynamics and erosion for small tube arrays in fluidized beds. In *Multiphase Transport and Particulate Phenomena* (Edited by T. Nejat Veziroglu), pp. 325–354. Hemisphere, New York (1989).
7. J. X. Bouillard and R. W. Lyczkowski, On the erosion of heat exchanger tube banks in fluidized bed combustors. In *Multiphase Transport and Particulate Phenomena* (Edited by T. Nejat Veziroglu), pp. 419–430. Hemisphere, New York (1989).
8. L. T. Fan, T. C. Ho, S. Hiraoka and W. P. Walawender, Pressure fluctuations in a fluidized bed, *A.I.Ch.E. Jl* **27**(3), 388–396 (1981).
9. G. Rudinger and A. Chang, Analysis of non-steady two-phase flow, *Physics Fluids* **7**, 1747–1754 (1964).
10. R. W. Lyczkowski, Transient propagation behavior of two-phase flow equations. In *Heat Transfer: Research and Application* (Edited by J. C. Chen), AIChE Symp. Series 75(174), pp. 165–174. American Institute of Chemical Engineers, New York (1978).
11. H. Tennekes and J. L. Lumley, *A First Course in Turbulence*, pp. 197–222. MIT Press, Cambridge, Massachusetts (1980).
12. T. W. Broadhurst and H. A. Becker, Measurement and spectral analysis of pressure fluctuations in slugging beds. In *Fluidization Technology* (Edited by D. L. Keairns), pp. 63–85. Hemisphere, Washington, DC (1976).
13. J. Verloop and P. M. Heertjes, Periodic pressure fluctuations in fluidized beds, *Chem. Engng Sci.* **29**, 1035 (1974).
14. J. R. Grace, Fluidized-bed hydrodynamics. In *Handbook of Multiphase Systems* (Edited by G. Hestroni), pp. 8-1 to 8-64. Hemisphere, Washington, DC (1982).
15. D. J. Needham and J. H. Merkin, The evolution of a two-dimensional small-amplitude voidage disturbance in a uniformly fluidized bed, *J. Engng Math.* **18**, 119–132 (1984).

DYNAMIQUE SPECTRALE PAR SIMULATION NUMERIQUE DE COMBUSTEURS BIDIMENSIONNELS A LIT FLUIDISE

Résumé—Le Laboratoire National Argonne a développé des méthodes pour étudier les phénomènes d'érosion dans les systèmes fluide/solides par intégration de l'état de l'art pour un modèle numérique hydrodynamique diphasique bidimensionnel (FLUFIX qui calcule les distributions temporelles et spatiales) avec érosion qui relie les propriétes hydrodynamiques calculées aux configurations et vitesses d'érosion. On rapporte ici une analyse spectrale qui corrèle la porosité, la pression et la vitesse dans le temps et l'espace pour un réacteur à lit fluidisé. Les principales fréquences des oscillations de porosité, de pression et de vitesse sont 0,7–4 Hz. Les oscillations de porosité et de pression se déplacent dans le combusteur à des vitesses de 0,4–1 m s^{-1}. Les oscillations de pression sont bien corrélées aux oscillations de porosité.

SPEKTRALE DYNAMIK IN SIMULIERTEN ZWEIDIMENSIONALEN WIRBELBETT-BRENNKAMMERN

Zusammenfassung—Am Argonne-National-Laboratory wurden Verfahren zur Untersuchung von Erosionsphänomenen in Fest/Flüssig-Systemen entwickelt. Zu diesem Zweck wird ein Rechenmodell (FLUFIX) zur Emittlung zeitlicher und räumlicher Verteilungen in zweidimensionalen Zweiphasenströmungen mit Erosions-Modellen verknüpft, welche die berechneten hydrodynamischen Eigenschaften mit Erosionsformen und -geschwindigkeiten verknüpfen. In der vorliegenden Arbeit wird über eine Spektralanalyse zur zeitlichen und räumlichen Beschreibung von Porosität, Druck und Geschwindigkeit in einer Wirbelbett-Brennkammer berichtet. Die wesentlichen Frequenzen der Porositäts-, Druck- und Geschwindigkeitsoszillationen liegen zwischen 0,7 und 4 Hz. Die Porositäts- und Druckoszillationen schreiten in der Brennkammer mit 0,4–1 m s^{-1} fort. Die Druckoszillationen lassen sich gut mit den phasenverschobenen Porositätsoszillationen korrelieren.

СПЕКТРАЛЬНАЯ ДИНАМИКА СМОДЕЛИРОВАННЫХ КОМПЬЮТЕРОМ ДВУМЕРНЫХ КАМЕР СГОРАНИЯ С КИПЯЩИМ СЛОЕМ И НЕСКОЛЬКИМИ ТРУБАМИ

Аннотация—В Национальной лаборатории Аргонна разработаны методы исследований явлений эрозии в системах жидкостей/твердых тел посредством двумерной вычислительной схемы FLUFIX, позволяющей рассчитывать временные и пространственные распределения, и моделей эрозии, устанавливающих зависимость между рассчитанными гидродинамическими свойствами и картиной и интенсивностью эрозии. В данном исследовании проводится спектральный анализ, устанавливающий временную и пространственную корреляцию порозности, давления и скорости типичной камеры с кипящим слоем и несколькими трубами. Основные частоты осцилляций порозности, давления и скорости составляли 0,7–4 Гц. Осцилляции порозности и давления перемещались в камере сгорания со скоростями 0,4–1 м $с^{-1}$. Существует тесная взаимосвязь между осцилляциями давления и запаздывающими осцилляциями порозности.